Available online at www.sciencedirect.com

ScienceDirect

Scripta Materialia 93 (2014) 24–27

Scripta MATERIALIA

www.elsevier.com/locate/scriptamat

Effect of pre-compressive treatment on creep behavior of a ⟨011⟩-oriented single-crystal Ni-based superalloy

Yong Su,[a,b] Sugui Tian,[a,*] Huichen Yu[c] and Lili Yu[a]

[a]*School of Materials Science and Engineering, Shenyang University of Technology, Shenyang 110870, People's Republic of China*
[b]*School of Energy and Power Engineering, Shenyang University of Chemical Technology, Shenyang 110142, People's Republic of China*
[c]*Beijing Key Laboratory of Aeronautical Materials Testing and Evaluation, Science and Technology on Advanced High Temperature Structural Materials Laboratory, AVIC Beijing Institute of Aeronautical Materials, Beijing 100095, People's Republic of China*

Received 3 August 2014; revised 15 August 2014; accepted 18 August 2014
Available online 2 September 2014

The effect of pre-compressive treatment on the steady-stage creep behavior of a ⟨011⟩-oriented single-crystal Ni-based superalloy was studied. Results show that pre-compression at 1040 °C/180 MPa along the [100] orientation improves the tensile creep strength of the alloy along the [011] orientation at 850 °C/400 MPa and 1040 °C/137 MPa. The elimination of gable channels, the relatively narrow roof channels and the more activated slip systems of dislocations are responsible for the better creep resistance of the pre-compressed alloy.

Keywords: Nickel alloys; Microstructure; Pre-compression; Creep; Dislocations

Single-crystal (SC) Ni-based superalloys have been widely used for producing turbine blades due to their excellent mechanical and creep properties at high temperatures [1,2]. Although SC blade parts in ⟨001⟩ orientation have been applied in aero-engines, it is difficult to ensure the exact orientation of SC superalloys, and misorientation of blade parts is unavoidable during the production process [3,4]. Moreover, the mechanical and creep properties of SC blade parts are inherently anisotropic, and the centrifugal force to which the parts are subject in service always deviates from the ⟨001⟩ orientation.

Some investigations indicate [5–8] that, compared to [001]-oriented SC superalloys, the [011]-oriented alloys display poor creep resistance at both intermediate and high temperatures [7,8], which is related both to the dislocation moving modes [9] and to the microstructure of the alloys [10]. Hence, under the combined action of the misorientation produced and the deviated centrifugal force, once the direction of the loads applied on blade parts is close to the [011] orientation, failure of the parts may rapidly occur, posing a severe risk to the turbine blades.

One of the most striking characters during high-temperature creep of SC superalloys is the rafting behavior of the γ′ strengthening phase. Some investigations have focussed on the γ′-phase pre-rafting treatment of [001]-oriented superalloys, which is found to have obvious effects on creep properties of the alloys [11–13]. However, the influence of γ′-phase pre-rafting on the creep properties of [011]-oriented SC Ni-based superalloys is still not clear.

In this paper, the γ′ phase in a [011]-oriented SC superalloy is pre-rafted along the [100] orientation, and the influence of the pre-rafting on the tensile creep properties of the alloy is investigated. New microstructural concepts combined with dislocation-slip characters are proposed to discuss the beneficial effects of the pre-rafting treatment, which are expected to provide the technical and theoretical basis for the development of turbine blades.

The preparation and other details of the [011]-oriented SC alloy studied in this paper were described elsewhere [14]. For in-depth comparative study, a [001]-oriented SC alloy with the same composition and heat-treatment regime is also prepared by the selecting crystal method, whose orientation is measured to be deviating by 7° from [001]. Methods for the creep-specimen preparation and microstructure observation of the two oriented alloys are reported in Refs. [14,15]. Some of the two oriented SC alloys are pre-compressed along the [100] orientation on the (100) plane at 1040 °C/180 MPa for 38 h. All creep tests for [011]-oriented alloy, whether pre-compressed or not, are along the [011] orientation, while those for the [001]-oriented alloy are along the [001] orientation.

Figure 1 shows the tensile creep curves of the alloys with/without pre-compression. Creep curves 1 and 2 in

* Corresponding author. Tel.: +86 24 25494089; fax: +86 24 25496768; e-mail: tiansugui2003@163.com

http://dx.doi.org/10.1016/j.scriptamat.2014.08.021
1359-6462/

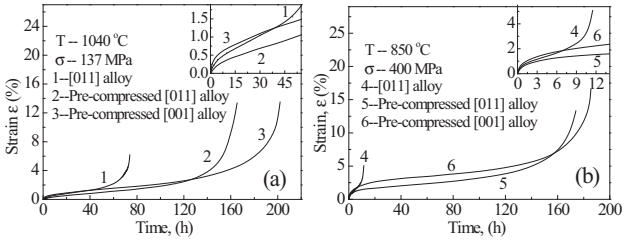

Figure 1. Creep curves of the SC Ni-based superalloys under different conditions: (a) 1040 °C/137 MPa, (b) 850 °C/400 MPa.

Figure 1a show that the creep life of the [0 1 1]-oriented superalloy at 1040 °C/137 MPa has been prolonged by 122.9% from 74 to 165 h after pre-compression, while creep curves 4 and 5 in Figure 1b indicate that the creep life of the alloy at 850 °C/400 MPa is increased more noticeably by 15 times from 11 to 174 h after pre-compression.

For comparative analysis, the creep curves of the pre-compressed [0 0 1]-oriented alloy under different conditions are also plotted, as marked by curves 3 and 6 in Figure 1, indicating that the pre-compressed [0 0 1]-oriented alloy has creep lives of 202 and 185 h at 1040 °C/137 MPa and 850 °C/400 MPa, respectively.

Figure 2 shows the microstructures in the interdendritic (top row) and dendritic regions (bottom row) of the [0 1 1]-oriented alloys at different states, indicating that during pre-compression and creep, the microstructure evolution results in a change in the size of the γ'/γ phases in the alloys, which is measured and listed in Table 1 (taking the (1 0 0) plane as the reference).

Figure 3 shows a schematic diagram of the microstructures in the [0 1 1]-oriented alloys at different states. Figure 3a schematically shows the microstructure in the alloy after full heat treatment (Microstructure I) based on Figure 1 in Ref. [14], indicating that Microstructure I comprises cuboidal γ' precipitates regularly arranged at a 45° angle relative to the [0 1 1] orientation. The $\gamma_{r(001)}$ and $\gamma_{r(010)}$ at 45° relative to the [0 1 1] orientation are called "roof channels", and the γ_g parallel to the (1 0 0) crystal plane are termed "gable channels" [7]. Based on Figure 2 in Ref. [14], Figure 3b schematically shows the microstructure of the [0 1 1]-oriented alloy without pre-compression after being crept for 40 h at 1040 °C/137 MPa (Microstructure II), indicating the γ' precipitates have transformed into one-dimensional stripe-like rafts during tensile creep.

Ignoring the heterogeneities of γ'/γ size between interdendritic/dendritic regions, Figure 2b shows that after pre-compression of the [0 1 1]-oriented alloy, most γ' precipitates display a particle-like configuration on the (1 0 0) plane. On the (0 1 1) plane (Fig. 2c), the γ' phase has transformed into a stripe-like rafted structure. The microstructure of the pre-compressed alloy on the $(0\,1\,\bar{1})$ plane is similar to that in Figure 2c, but has been omitted here. It can be concluded that after pre-compression, the cuboidal γ' phase in the [0 1 1] alloy has transformed into P-type rafted structure along the [1 0 0] orientation, as schematically shown in Figure 3c (Microstructure III). In fact, after being crept for 60 h at 1040 °C/137 MPa, the formed microstructure in the pre-compressed [0 1 1]-oriented alloy (Microstructure IV) is similar to Microstructure III, and hence Figure 3c represents Microstructures III and IV in this study, for which the difference in size of the γ'/γ phases is listed in Table 1.

In this study, for the [0 1 1]-oriented alloys with/without pre-compression, we mainly focus on the creep behavior at steady-state stage, and the cutting of γ' rafts is not considered. Dislocation slip, cross-slip and climb in γ' channels are thought to be the main deformation mechanisms for the alloys, and are mostly concentrated in "roof" channels [7].

For Microstructure I, when load is applied along the [0 1 1] orientation, four equivalent slip systems with Schmid factors of 0.408 are mainly activated, $(1\,1\,1)[1\,\bar{1}\,0]$, $(\bar{1}\,1\,1)[1\,1\,0]$, $(1\,1\,1)[\bar{1}\,0\,1]$ and $(\bar{1}\,1\,1)[1\,0\,1]$ [16], of which the first two are mainly activated in $\gamma_{r(001)}$, while the latter two are mainly activated in $\gamma_{r(010)}$. The lower number of slip systems activated during creep of the [0 1 1]-oriented alloy is one of the main reasons for it having worse creep resistance than the [0 0 1]-oriented alloy resulting in the poor strain-hardening effects [17].

Compared to Microstructure I, Microstructure III is significantly changed.

First, γ_g has been eliminated, so the dislocation movements there are eliminated.

Secondly, $\gamma_{r(001)}$ and $\gamma_{r(010)}$ still exist, but $\gamma_{r(001)}$ and $\gamma_{r(010)}$ are often blocked by the plate-like γ' rafts due to the lateral connection of them along the [0 1 0] and [0 0 1] orientations (see arrows 1 and 2 in Fig. 2b, and the region enclosed by dashed lines in Fig. 3c). This labyrinth-like microstructure forces dislocations to change their moving direction constantly, and is beneficial to enhancing the dislocation-moving resistance and improving the creep strength of the alloy [18].

Thirdly, although the average widths of the γ channels (75/70 nm in interdendritic/dendritic regions, Table 1) in Microstructure III are larger than those (52/49 nm in the corresponding regions) in Microstructure I, there are two points worth noting. (i) The width of the γ channels in Microstructure III is not homogeneous, and many micro-bottleneck-like channels form due to the lateral growth of γ' rafts (see arrows 3 and 4 in Fig. 2b). (ii) The widths of the γ' rafts in Microstructure III (760/650 nm in interdendritic/dendritic regions) are much larger than those (420/390 nm in the corresponding regions) in Microstructure I. The beneficial effect of the above two points on the creep resistance will be discussed in more detail below.

These above three aspects may account for the lower creep rate and creep strain of the pre-compressed [0 1 1]-oriented superalloy during primary creep both at 1040 °C/137 MPa and 850 °C/400 MPa (see inserts in Fig. 1a and b).

As for Microstructures II and IV, there are two characteristics worthy of attention.

First, the widths of $\gamma_{r(010)}$ or $\gamma_{r(001)}$ (157/125 nm in interdendritic/dendritic regions) in Microstructure IV are less than half of those of $\gamma_{r(010)}$ (400/290 nm in the corresponding regions) in Microstructure II. Moreover, the widths of the γ' rafts (850/750 nm in interdendritic/dendritic regions) in Microstructure IV are obviously larger than those (450/320 nm in the corresponding regions) in Microstructure II. Moreover, in Microstructure IV, the labyrinth-like microstructure is retained (Figs. 2e and 3c). Considering the common $\gamma_{r(010)}$ in Microstructures II and IV, without loss of generality, we take the slip system $(1\,1\,1)[\bar{1}\,0\,1]$ in $\gamma_{r(010)}$ as an example to explain the dislocation movements in the matrix channels, as shown in Figure 4a. In this figure, the segments AB, BC and CD represent the glide, bowing out and climb of dislocations. After climb, dislocations go on gliding in γ channels, as marked by DE. When facing